# Adsorption of a Laccase from *Fusarium Proliferatum* on Au(111) and HOPG Electrodes: a Scanning Probe Microscopy and Electrochemical Approach

*K. González Arzola[1], A. González Orive[2], M.C. Arévalo[2], L. Vázquez[3], A. Hernández Creus[2], M.A. Falcón[1,*]*

[1] Departamento de Microbiología y Biología Celular. Facultad de Farmacia. Universidad de La Laguna. 38206. Tenerife, Spain.
[2] Departamento de Química Física. Facultad de Química. Universidad de La Laguna. 38206. Tenerife, Spain.
[3] Departamento de Física e Ingeniería de Superficies, Instituto de Ciencia de Materiales de Madrid, C.S.I.C., Cantoblanco, 28049. Madrid, Spain.
[*]E-mail: mafalcon@ull.es

A laccase enzyme produced by *Fusarium proliferatum* was successfully adsorbed as a laccase submonolayer (SML) on a bare Au(111) single-crystal electrode (Au), the same electrode modified with a hexadecanethiol self-assembled monolayer (SAM-Au) then treated with the SML, and also on a highly-ordered pyrolytic graphite electrode (HOPG). The three treated electrode surfaces were scanned by AFM and STM, and their electrochemical and catalytic responses studied. The SML clearly established electrical contact with Au, but did not retain either electrochemical response or catalytic activity. However, the SML on SAM-Au and HOPG surfaces showed a direct electron transfer (DET) process, retaining catalytic activity. The arrangement and electrochemical and catalytic behavior of the SML on the different surfaces are clearly linked with their interactions with the surfaces, without evidence of dependence on any specific molecular orientation. Alternative explanations for this are provided, given the possible conformational differences resulting from these interactions, which would alter the internal electron transfer mechanism at the laccase active centers.

## 1. INTRODUCTION

Most laccases (benzenediol: oxygen oxidoreductases, EC 1.10.3.2) are members of the multi-copper-oxidase enzyme family and catalyze the direct four-electron reduction of $O_2$ to $H_2O$, without

producing highly toxic reactive oxygen species [1, 2]. Devices constructed with these enzymes directly bonded to the electrode surfaces show excellent potential for future miniaturization, to produce extremely selective, sensitive and simple analytical systems [3]. An important biotechnological goal is therefore to understand the electrochemical reactions of redox proteins, principally in order to control their interactions with electrode surfaces [4]. Adsorption of proteins on a solid surface involves a complex set of interactions, whose elucidation becomes essential in the rational design of solid-support surfaces for biotechnological and biomedical applications [5]. For example, retention of native-like structure, long shelf-life, and a high yield of biological activity of the bound enzyme are highly desirable. Controlling these attributes continues to be a challenge, and there are no specific rules or guidelines as to how this can be achieved for a given enzyme and solid support. Moreover, the understanding of protein-solid interactions is still primitive and most of the biomolecules bonded in this way are easily deactivated by certain changes in their environment and functionality [5]. The latter is affected by the molecular orientation, mainly driven by the specific molecular interactions with the neighboring molecules. Therefore, during the process of the thin-layer formation, the protein molecules should be immobilized to maintain their orientation without loss of specific functionality [6].

Some researchers have suggested that laccase molecules are oriented differently when adsorbed on gold or carbon surfaces [7, 8]. These authors proposed that laccase is oriented with the T2/T3 copper cluster facing the gold electrode, while on carbon surfaces it lies in direct electron contact with the T1 copper site. The orientation of laccase with respect to the T2-T3 copper cluster may explain the negligible direct electron-transfer (DET) based catalysis of $O_2$ electroreduction by bilirubin oxidase or laccase, when they are directly bound on gold [7, 9]. However, in a more recent study with bilirubin oxidase [10] it was concluded that the enzyme adopts a spread of slightly different micro-orientations that place its electron entry/exit site at a certain distance from the electrode surface at which the catalytic process of the enzyme can reach its maximal efficiency. Moreover, since several different redox potentials ($E^0$) are expected for the structurally different T2/T3 cluster intermediates [11-14], a catalytically inactive low redox-potential resting-form of the T2/T3 copper cluster could also be formed when laccase is adsorbed on gold, which might have a very slow intra-molecular electron transfer (IET) rate, analogously with resting-forms of the laccases in their catalytic cycle (turnover) [12, 15, 16]. As a result, a low or null driving force for the electron transfer process would be expected [9]. Thus, there is an uphill gradient in the IET from the T1 ($E^0 \sim 750$ mV vs. NHE) to the T2/T3 cluster ($E^0 \sim 400$ mV vs. NHE), allowing this resting-form to have such a slow electron transfer rate.

On the other hand, the inhibition of enzymatic catalysis in the presence of $OH^-$ and $F^-$ ions, and by target laccase substrates when added at a high concentration, is due to changes caused in the chemical and electronic structure of the T2-T3 cluster in the presence of such compounds [3, 8, 11, 15, 17]. These authors suggest that different intermediate forms of the enzyme are generated. As a result, such a low or zero driving force could indeed be expected, as normally occurs in the enzyme turnover; consequently its catalytic activity may be partially or completely inhibited.

To the best of our knowledge studies that characterize the laccase submonolayer (SML) on electrodes are extremely scarce. Klis et al. [4] studied the structure of a *Cerrena unicolor* laccase

submonolayer on modified gold by Scanning Tunneling Microscopy (STM), concluding that the blue copper site is conserved in the protein when immobilized by organothiol monolayers and that the catalytic efficiency of the laccase remain only when the enzyme have not direct contact with gold. No explanation was given.

Apparently, the only way the orientations of an adsorbed asymmetric molecule can so far be detected is by constructing nanostructural laccase SML. Consequently, the aim of this paper is to characterize the laccase SML on Au, hexadecanethiol self-assembled monolayer (SAM-Au) and highly-ordered pyrolytic graphite electrode (HOPG) surfaces, using Atomic Force Microscopy (AFM) and STM, comparing these results on the layers' structure with their catalytic and electrochemical behavior. In a recent report we immobilized this laccase to form multi-layers on HOPG and gold electrodes without linkers, successfully producing images of single laccase molecules 5-6 nm long by AFM [18]. The enzymatic activity was retained to a significant extent toward both oxidation of the target substrate violuric acid and oxygen reduction at HOPG electrodes, but was negligible at gold electrodes. In this paper, we study the DET reactions between the laccase molecules in close contact with the electrodes, taking into account the redox conversion of their copper center under anaerobic conditions, as a test to evaluate the DET reactions of the enzyme close to the electrode. This ensemble of data has led us to rational explanations of the characteristics of the laccase layers and their catalytic and electrochemical properties, in regard to the different interactions between the enzyme and the surface of the electrodes used. Importantly, this enzyme is a novel high redox-potential fungal laccase from *Fusarium proliferatum* ($E^0$ 750 mV vs. NHE) [18], which is endowed with properties useful for biotechnological applications, such as its stability against temperature and in a very wide pH range [2].

# 2. EXPERIMENTAL PART

## 2.1. Chemicals

Citric acid monohydrate, disodium hydrogen phosphate dehydrate, trisodium citrate and phosphoric acid were supplied by Scharlau Chemie. 2,6-dimethoxyphenol and hexadecanethiol were purchased from Aldrich Chemical Co. Potassium phosphate, tartaric acid, 2,2'-azino-bis (3-ethylbenzothiazoline-6 sulfonic acid (ABTS) and electrophoresis reagents were from Sigma (St. Louis, Mo.). NaOH, AgNO$_3$, HCl and ethanol were acquired from Panreac, while NaCl and KCl were from Merck. All these reagents were analytical grade and utilized without further purification.

## 2.2. Laccase purification

A ligninolytic *Fusarium proliferatum* strain (MUCL 31970) [19] was used as laccase source. The fungus culture to produce the laccase enzyme, the initial purification of this enzyme and the HPLC equipment  used to obtain the crude laccase extract is described elsewhere [20].  The following steps were performed to purify the enzyme up to electrophoretic homogeneity. The active fractions obtained from the first purification step [20] were pooled (8 mL) and then dialyzed against 66 mM Sørensen

buffer at pH 7.4 and concentrated by Amicon (50 kDa cut-off). One aliquot (1mL 7 μg proteins) was then loaded into an ion-exchange mono Q H/R 5/5 column (5×50 mm, Pharmacia) and equilibrated with the buffer and eluted at a flow rate of 1 mL min$^{-1}$. Laccase activity was eluted in a nonlinear gradient of 0–0.2M NaCl in the same buffer. The fractions were checked with ABTS, and those with activity pooled and dialyzed against distilled water. Samples containing 50 μg protein were freeze-dried and kept at −80°C. Afterwards, these aliquots were diluted in 66 mM Sørensen buffer, pH 7, containing 0.2 M NaCl and applied (200 μL; 10 μg mL$^{-1}$) to a Superdex 75 column (10/30, Pharmacia) at a flow rate of 0.8 mL min$^{-1}$. Fractions (0.8 mL) were collected, and those with activity against ABTS were dialyzed against distilled water and freeze-dried for further utilization. During the purification process, PAGE (polyacrylamide gel electrophoresis) was performed as described elsewhere [21] to check the purity of the enzyme reached in the last purification step indicated above. Protein bands were developed by silver staining (Bio-Rad) and zymograms by ABTS (5 mM) in McIlvaine buffer (0.1 M citric acid − 0.2 M disodium hydrogen phosphate) at pH 4.5. Protein content was determined spectrophotometrically at 595 nm with the Coomassie Blue method [22] using bovine albumin fraction V as protein standard (Bio-Rad protein assay).


*2.3. AFM/STM microscopy*


AFM operating in tapping mode (a Multimode microscope equipped with a Nanoscope V controller from Digital Instrument/Bruker) was used to scan the different layers, in air and under liquid (Milli-Q water or 10 mM phosphoric acid-sodium hydroxide buffer at pH 6) at room temperature. Standard (spring constant in the 20-80 N m$^{-1}$ range) and softer (1-5 N m$^{-1}$) silicon cantilevers were employed for measurements in air. Special care was taken to minimize the protein deformation by the tip load. For measurements under liquid, 0.38 N m$^{-1}$ cantilevers were used. STM Images were made only after thermal equilibrium was reached, with a Digital Instrument Nanoscope IIE microscope, operating in air in constant current mode. Pt/Ir commercial tips were used, with tunneling currents between 0.2-0.5 nA and bias potentials of 250 to 650 mV. An evaporated gold layer (250 nm thick), flame annealed on 1 cm$^2$ chromium-coated glass plates (Arrandee™) and 1 cm$^2$ freshly cleaved HOPG (basal plane) were used as substrates. Calibration of AFM and STM piezotubes was performed by obtaining the atomic resolution of HOPG and the height of monatomic Au steps. Some of the images were analyzed using WSxM software (free from http://www.nanotec.es) [23].

Laccase SML on Au were prepared by dropping 25 μL of a pure laccase solution (0.012 μg mL$^{-1}$, approximately 2 x 10$^{-10}$ M, to ensure providing a submonolayer) on the gold plate for only 2 minutes. Then the plates were thoroughly rinsed in high purity water. Similarly, aliquots (25 μL) of pure laccase solution were dropped overnight avoiding solvent evaporation on a freshly cleaved HOPG surface, and then rinsed. Those specimens to be scanned under liquids were protected under a buffer drop. Bare Au(111) single-crystal electrode (Au) plates were also modified with a self-assembled monolayer of hexadecanethiol (HDT) before adding the enzyme to obtain a Au(111) single crystal electrode modified with a hexadecanethiol self-assembled monolayer (SAM-Au). The SAM-Au was prepared by dipping an Au plate into 1 mM HDT ethanol solution for 24 hours, preventing ethanol

evaporation. Subsequently, it was thoroughly washed in ethanol and left to dry for 24 hours in a desiccator. This process gave rise to a surface covered with a 2.1 nm thick SAM of HDT. Finally, we proceeded to adsorb laccase onto the SAM-Au in the same way as the HOPG. The SML appearing on the respective surfaces were the same in all the assays repeated under each of these conditions.

### *2.4. Determination of catalytic activity*

The catalytic activity of a laccase SML placed on Au, SAM-Au and HOPG electrodes was evaluated by studying the oxidation of 2,6 dimethoxyphenol (DMP) by spectrophotometry using a modified assay as previously described [24], by monitoring oxidation of DMP ($\varepsilon_{468}$ 10,000 M$^{-1}$ cm$^{-1}$). To this end, the surfaces of Au, SAM-Au and HOPG were modified with laccase as indicated above. Subsequently, the three surfaces were immersed in a solution containing 10 mL of sodium tartrate buffer (0.5 M tartaric acid-sodium hydroxide) adjusted to pH 4.5 and 4 mM DMP at 37 °C, with agitation (70 rpm, IKA Labortechnik KS501) for 48 hours. Samples (1 mL) of these solutions were taken at 6, 24, 36 and 48 h, and absorbance at 468 nm, determined using a UV-VIS spectrophotometer (Beckman Coulter DU 800). To test the DMP stability during the assay, controls as described above but without enzyme were incubated during the same time periods.

### *2.5. Electrochemical measurements*

The electrochemical measurements were conducted at room temperature in a specially designed 0.5 mL electrochemical cell in which only the HOPG basal plane or the gold surfaces were in contact with the solution. It was adapted for 1 cm$^2$ surface-area working electrode plates, using a potentiostat-galvanostat (EG&G PARC mod. 273A). An Ag/AgCl/KCl 3M (211 mV vs. NHE) electrode was used as reference electrode to which scale all the potentials refer in the text, and a Pt ring as counter-electrode. Au and HOPG were employed as working electrodes. The supporting electrolyte solution was McIlvaine buffer adjusted to pH 6.

Laccase SMLS were prepared as already indicated for AFM/STM imaging. Electrochemical responses of bare and laccase-modified electrodes were measured by cyclic voltammetry at 0.050 V s$^{-1}$, between 0 and 0.750 V.

## 3. RESULTS AND DISCUSSION

### *3.1. AFM and STM characterization of laccase adsorbed on Au and HOPG surfaces*

Figure 1A shows the AFM image obtained in air of a laccase SML adsorbed on Au after incubating 25 µL laccase solution for 2 min on an Au plate; and Fig. 1B, the AFM image obtained in liquid of a similar sample. AFM characterization of SML in liquid revealed an *in situ* protein-electrode morphology more like that found for free laccase. Under both conditions, laccase molecules tend to cover most of the surface in a short period of time (2 min).
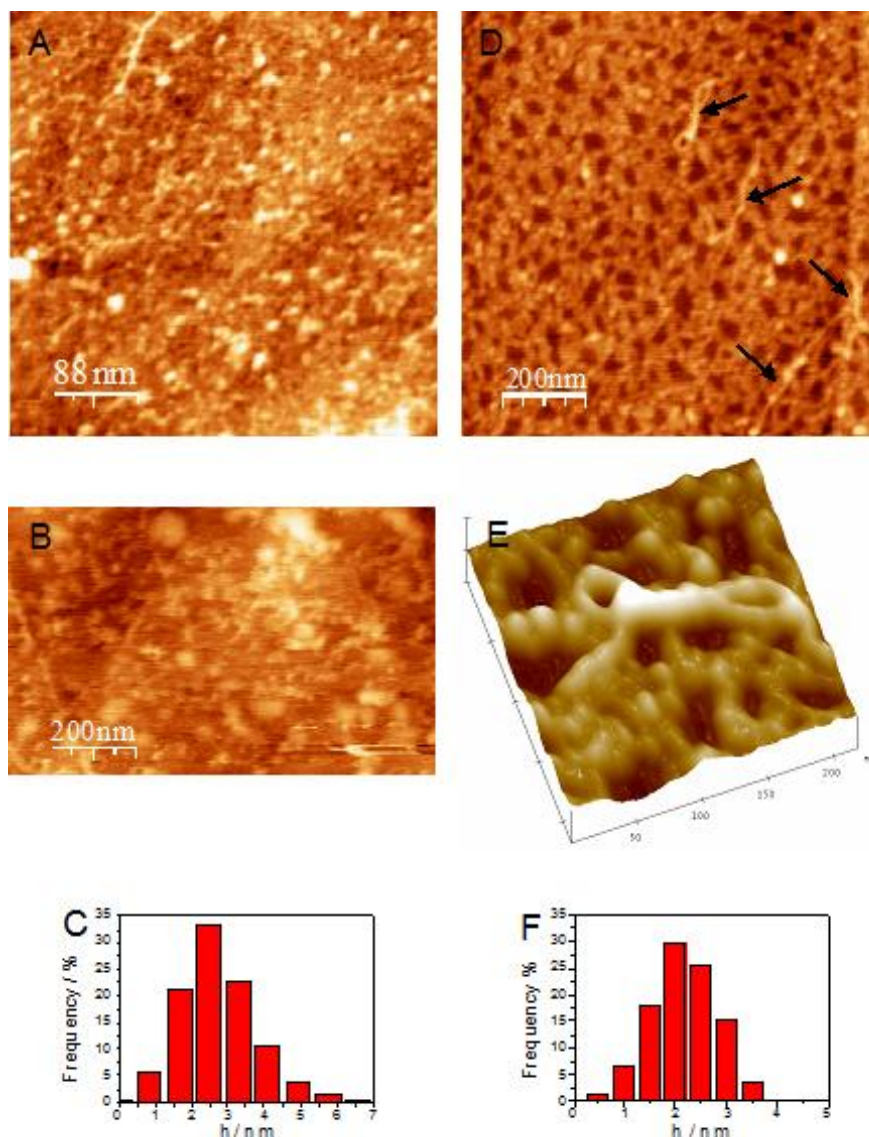
**Figure 1.** AFM images of a laccase SML on Au and HOPG. (A) Au in air, 425 nm x 425 nm; (B) Au in phosphate buffer solution (pH 6), 1 μm x 0.5 μm; (C) height histogram corresponding to a laccase SML obtained on Au; (D) laccase SML obtained on HOPG, 1 μm x 1 μm; the arrows point to some nanowires; (E) 3D detailed view (220 nm x 220 nm) of Fig. 1D; (F) height histogram corresponding to the laccase SML obtained on HOPG.

Bearing in mind the very low laccase concentration ($2x10^{-10}$ M, about $5x10^8$ molecules), formation of single laccase molecules could easily be expected. However, due to the rapid and intense laccase-gold interaction and the strong tendency of these molecules to link to each other spontaneously and rapidly, images of single molecules were difficult to obtain. So, under our assay conditions, laccase aggregates in a wide range of sizes were detected (Fig. 1B). Interestingly, the height histogram obtained in all samples, both in air and liquid conditions, shows that these particles, independently of the molecules' association, were always 2.5 nm high (Fig. 1C). In contrast to Au surfaces, laccase molecules are adsorbed rather slowly onto HOPG, and under our conditions several hours were necessary to form a laccase layer. Fig. 1D shows the AFM image in air after incubating 25 μL $2x10^{-10}$

M laccase solution on HOPG for several hours, preventing solvent evaporation. As can be seen, the molecules built up a complex branched network, with many randomly distributed voids of bare HOPG (about 50 nm wide) where atomic resolution of carbon was easily attained. Similar branches and networks were also seen when using a more concentrated laccase solution [18]. When laccase-modified HOPG was scanned by AFM under liquid conditions, an analogous branched layout of laccase molecules to those in air was also observed (data not shown). Nevertheless it should be noted that while laccase multilayers were easily obtained on gold [18], on HOPG surfaces a complete laccase monolayer was never obtained (independently of the incubation time or the laccase concentration) because the strong molecule-molecule interaction immediately gives rise to 3D structures, always leaving large voids of free graphite on the surface (Fig. 1E). The height of these particles was again ≈2.5 nm high (Fig. 1F).

The results commented are corroborated in Fig. 2 in which a long scale cross section analysis is performed. Thus, it can be seen than on both electrodes and under all experimental conditions laccase molecules are always lying in flat giving ≈2.5 nm high. Thus, Fig. 2A-B shows in detail how the laccase SML on Au was formed by molecules clustered into rounded 2D islands, very different in size. Although most of these 2D islands were less than 30 nm long, some of them were as long as 100 nm in width but less than 2.5 nm in height (h) (Fig. 2B). At greater scales (Fig. 2C-D), the laccase SML on Au clearly left voids up to 2 nm deep of bare gold surface, easily detected everywhere. The larger-scale AFM image (Fig. 2E-F) shows the laccase SML on HOPG in greater detail. Again the cross-section analysis is the same as for Au (Fig. 2C-D)

Since most laccase molecules contain 4 Cu atoms [11], they can easily be scanned by STM. Fig. 2G-H shows the STM image of some single laccase molecules adsorbed on the Au surface and their cross-section with a lateral length (size) around 5-6 nm. Whereas STM images of laccase molecules adsorbed on Au were easy to obtain, their interaction on the HOPG surface was too weak to be scanned and they were continuously swept away by the STM tip. Since the STM senses the electron density of the molecules and not the real topographic profile, the z scale in Fig. 2G-H is practically ten times lower than the real height of the laccase molecule.

Thus, laccase SML layers on HOPG can be said to be oriented in the same way as on Au. Moreover, the mean height measured in all conditions (2.5 nm) is not even half the maximum size of the molecule (about 5-6 nm). This indicates that the laccase molecules are lying flat along their longest axis under all the conditions assayed. These measurements are in agreement with the size we found for this laccase (6 nm by AFM) in a previous report [18] and those reported for many other laccases using AFM and STM [4, 25, 26]. Some values for different laccase monomers estimated by X-ray crystallography [27-33] are as high as 7 nm.

The different aggregation patterns and adsorption dynamics observed on the two surfaces suggest a very different laccase adsorption mechanism on HOPG from that on Au. Given the lower reactivity of carbon, the laccase-laccase interaction can be expected to be much stronger than that with the HOPG surface. Therefore, it should indeed promote the growth of large three-dimensional branched structures of protein molecules on HOPG (compare previous results [18] and Fig. 1E). Contrastingly, the hydrophilic gold surface interacts strongly with laccase molecules, allowing the rapid formation in about 2 min of a compact uniform layer, well adhered to the surface (Fig. 1A).
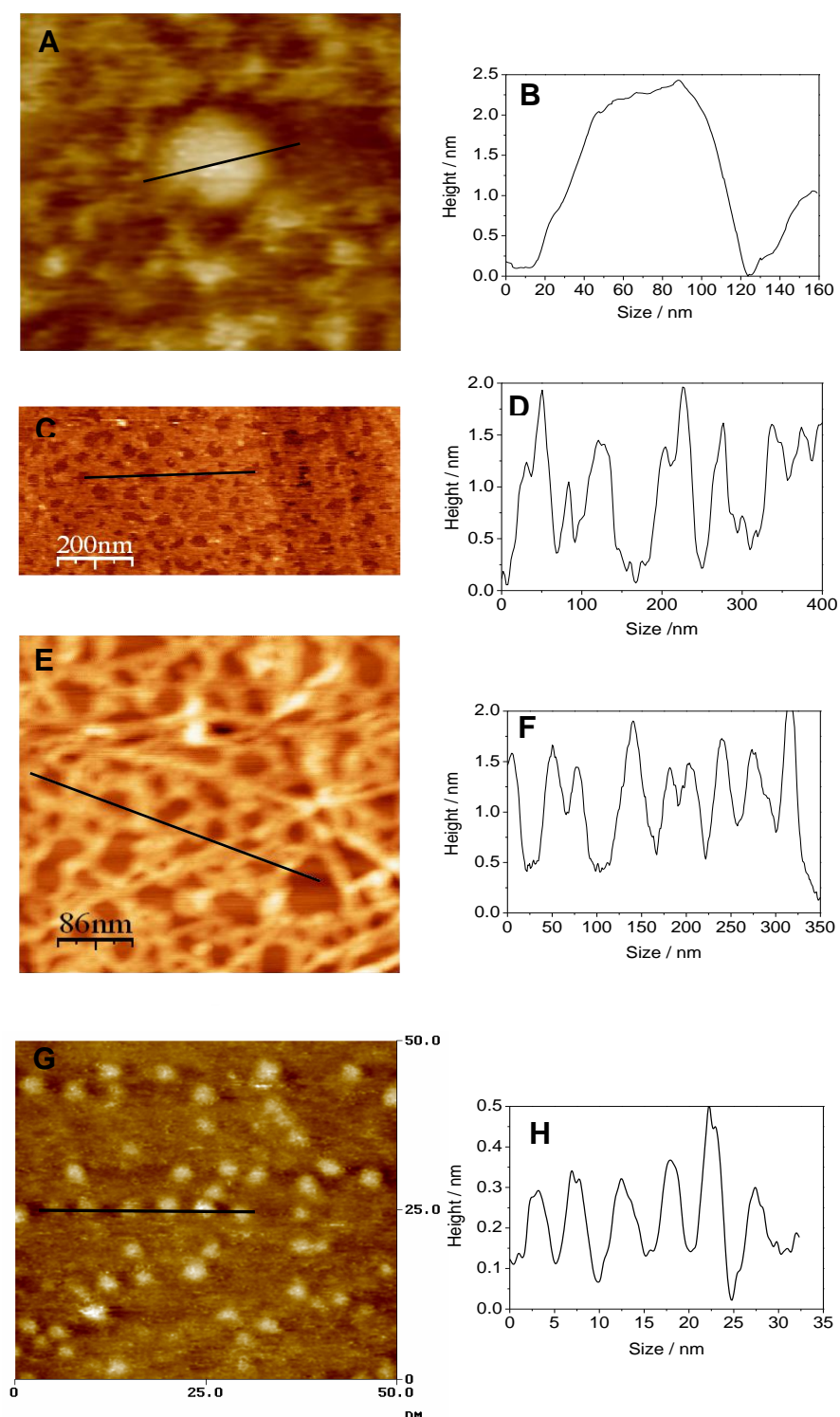
**Figure 2.** AFM (A, C, E) and STM images (G) and their corresponding cross section analysis (B, D, F, H) along the black line, for laccase SML adsorbed on Au and HOPG surfaces. (A) Au in liquid, 300 nm x 300 nm; (C) Au in liquid, 1000 nm x 500 nm; (E) HOPG in air 430 nm x 430 nm; (G) Au in air, 50 nm x 50 nm.

Since the experiments in high ionic strength medium (1M KCl) showed no alteration at all in the results (data not shown), interactions other than electrostatic forces must be linking the enzyme with both electrode surfaces. Importantly, the images obtained in liquid and air on both surfaces (Au

and HOPG) do not support a different orientation of the laccase, as widely accepted in previous studies [3, 9, 34, 35]. However, our study could back up the suggestion made by other authors for bilirubin oxidase [10] or even for laccase [36], based on structural considerations, that certain microorientations of Type 1 Cu close to the electrode surfaces provide faster electron transfer, thus improving enzymatic properties like catalytic efficiency, stability, etc.

The AFM/STM study presented here does not allow further elucidation of this particular topic. Moreover, the rapid adsorption of laccase SML on Au (2 min) points to a rapid chemical reaction between the enzyme and gold. It could be largely mediated by the free amine and especially the sulfhydryl groups which interact covalently with the gold [37]. Consequently a severe alteration in its molecular flexibility might occur, involving other changes such as loss of catalytic activity. This tentative explanation receives greater support in the electrochemical and catalytic assays reported below.
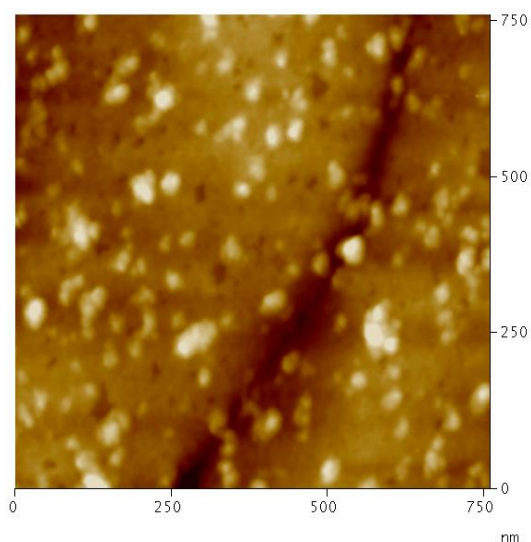


**Figure 3.** AFM image (760 nm x 760 nm) after the adsorption of 25 µL 0.012 µg mL$^{-1}$ laccase solution on a SAM-Au surface. Laccase aggregates appear randomly distributed as bright spots on top of the SAM-Au. Their sizes vary widely.

In a previous study [10], modification of electrode surfaces with linkers containing a carboxylate group located on an aromatic protrusion has been shown to be useful for binding multicopper oxidases in an orientation allowing fast electron transfer. In the present work, in order to explore the hypothesis described earlier, and achieve a more "graphite like" hydrophobic surface, we have modified the gold surface with a long-chain (C16) alkanethiol self-assembled monolayer (2.1 nm thick) and a non-polar group terminating the thiol (CH$_3$). In this way, the strong interaction between gold and laccase molecules can be easily avoided. Consequently, an enzyme distribution pattern like that on HOPG could be expected. Fig. 3 shows the corresponding AFM image in air of a SAM-Au, after several hours in contact with a dilute laccase solution. Indeed, the image resembles those obtained on HOPG. Thus, many 3D laccase aggregates appear randomly distributed, leaving large areas where the SAM-Au surface can be seen. This would confirm the prevalence of weak van der Waals

interactions instead of the stronger interaction attributed to laccase-gold adsorption in this study. Likewise, a gold grain border and small holes (dark spots) in the SAM-Au monolayer are also seen in this figure.

Adsorption of proteins on solid surfaces comprises a set of interactions via mechanisms too complex to elucidate [5]. It was previously proposed that organic molecules endowed with amino groups (alkyl amine or epoxy amine) interact with unmodified (bare) gold surfaces through covalent coordination bonds [38-42]. Furthermore, the laccase from *Trametes versicolor* was shown to be immobilized on a nanoporous gold surface by covalent interaction between its amino groups and the gold [37]. This strong gold-amino interaction appears to give rise to highly stable compact laccase layers, like those we describe elsewhere [18], and could similarly support the formation of the laccase SML described in this study. In contrast, the weak interactions between the carbon surface and the protein should facilitate laccase-laccase aggregation, leaving voids on HOPG as commented above (Fig. 1D, E).

The laccase SML on all the above surfaces may therefore be formed by the different adhesion mechanisms between the electrode and the enzyme. In this case, its different kind of interaction with gold or carbon could lead to a different reactivity when adhered on these surfaces. We therefore decided to study for the first time the catalytic and electrochemical behavior of this laccase SML on Au and HOPG, comparing it with that on gold covered with HDT, to avoid the direct link between the electrode surface and the protein.

*3.2 Catalytic activity of laccase SML on Au, SAM-Au and HOPG*

As mentioned previously, we showed that a multi-layer laccase gave electrochemical signals on both gold and carbon electrodes [18]. Furthermore, the enzyme retained its catalytic activity against laccase target substrates and reduced oxygen through a DET mechanism when adsorbed on carbon electrodes, these processes being negligible on Au [18]. We then checked what occurs with the catalytic and electrochemical properties of a laccase SML.

In order to study the catalytic activity of laccase SML, the oxidation of a laccase substrate (DMP) was monitored according to the increments in absorbance values at 468 nm. The reaction was maintained for a long period (48 h) because of the slow reaction rate, caused by the low laccase concentration (maximum 0.3 ng) in the SML. Due to the long incubation period of the assays, exhaustive controls for each experiment using the same surfaces incubated in the presence of DMP were carried out without laccase. No spontaneous DMP oxidation was detected during the incubation period (data not shown).

As can be seen in Fig. 4, the laccase molecules adsorbed on the HOPG surface oxidized DMP, as detected by a increase in absorbance at 468 nm. In contrast, laccase molecules were much less effective in oxidizing DMP on the Au surface, with an activity 7.5 times lower than on HOPG (Fig. 4). Indeed, laccase on Au attains a constant negligible activity maintained during all the incubation period (Fig. 4). It is a well-known fact the presence of residual activity of adsorbed laccase on different surfaces even if significant denaturation of the enzyme occurs. Interestingly, it must be mentioned that

the Au surface was 90-95% covered, compared to 70-75% on HOPG (see Fig. 1 A,D). On the other hand, the laccase adsorbed on SAM-Au recovered up to about 50% of the enzymatic activity detected on HOPG. In contrast to that happen on gold, laccase activity rises continually on SAM-Au, (Fig. 4).

The great variation in catalytic efficiency between the laccase SML adsorbed on the different surfaces could be explained by the possible alterations in its molecular flexibility or its catalytic center micro- structure which is capable of binding ligands. These factors should mainly affect the laccase molecules directly adsorbed on Au. In addition, considering the molecular mechanism of the IET at the active site of multicopper oxidases [3, 9, 34, 43-45], conformational changes in the protein would affect this process, called the "hopping" mechanism [11, 46-48]. Some authors report that this mechanism is blocked under certain conditions, for example, in high concentrations of target substrate [3, 43] or OH⁻, F⁻, NO and $H_2O_2$ [45], and propose that an alternative "non-hopping" route operates under these conditions. As a consequence, a great or complete loss of catalytic activity is known to occur, as here detected when the laccase is adsorbed on Au (Fig. 4). On the other hand, because of the weak interaction with HOPG, although the enzyme must maintain multiple attaching points (e.g. hydrogen bonds) it should allow the enzyme to conserve a conformational status similar to that of the free enzyme, thus retaining its catalytic activity (Fig. 4 black circles). A similar explanation can be given when laccase is bound on SAM-modified Au (Fig. 4, black squares).
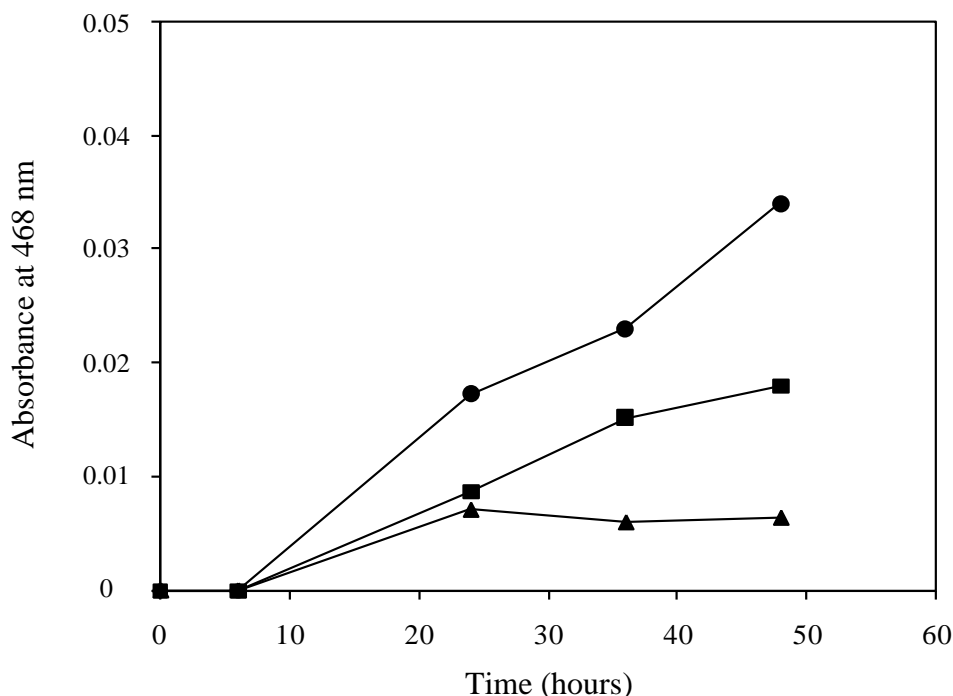


**Figure 4.** Increases in the absorbance values at 468 nm vs. time (hours) for laccase adsorbed on Au (▲), SAM-Au (■) and HOPG (●).

*3.3. Electrochemical response of laccase SML on Au, SAM-Au and HOPG*

Fig. 5A shows the cyclic voltammograms (CV) obtained on Au in buffer solution (dotted line) and after adding 25 μL 0.012 μg mL⁻¹ laccase solution on Au. Fig. 5B shows the corresponding result

obtained for a laccase SML deposited on HOPG; and Fig. 5C, on SAM-Au. In Fig. 5A, the characteristic waves reflecting the formation and reduction of gold oxide (dotted line) proved to be totally inhibited after laccase SML adsorption (solid trace), showing non-voltammetric peaks in the studied potential range -0.2 to 0.8V.

Therefore, the laccase SML must be covering the entire gold surface, which supports the AFM studies discussed before. Furthermore, this contrasts with the CVs registered for a laccase multilayer adsorbed on Au, which yielded a well-defined anodic peak at 350 mV vs. SCE [18]. However, when an equivalent quantity of enzyme is set on HOPG, an anodic peak potential ($E$a) is detected at about 600 mV vs. Ag/AgCl.

This value is close to those detected for the $E$a on HOPG and glassy carbon electrodes modified with a laccase multilayer (660 mV vs. SCE) [18], and also equivalent to those by square-wave voltammetry 625 mV vs. SCE [18]). These values were attributed to the T1 active center, despite the difference found when calculated by titration (510 mV vs. SCE) [18]. This different behavior of the laccase SML confirms the strong enzyme-gold interaction of the laccase molecules in direct contact with the gold surface, which probably displaced the enzyme's electrochemical response to much more positive values.

From the results discussed in this section, it is evident that although the enzyme is set on both surfaces in the same way and no preferential orientation is detected by AFM/STM studies, the SML electrochemical behavior on the two surfaces is different.

In this regard, adsorbed laccase molecules may well undergo the above conformational changes and their functionality would be severely impaired, as proposed for ceruloplasmin covalently bound to gold [44]. This damage somehow impedes the normal internal electron transfer or involves a decrease in the kinetics of the redox center reaction, so blocking the detection of electrochemical signals corresponding to the T1 or T2/T3 cluster, as here shown (Fig. 5A). The electrochemical respond shown in Fig.5, are    representative enough taking into account that our systems correspond to a laccase SML adsorbed. This behavior is in good agreement with a similar study [4]. Nevertheless, our results contrasts with those described by several authors using multi-layers of different multicopper oxidases and bare or modified gold electrodes [7, 9, 18, 35].

In the opposite scenario, the laccase SML physically adsorbed on HOPG can be oxidized under anaerobic conditions on the electrode surface, with a clear anodic wave that starts at about 400 mV and shows a rather poorly defined current maximum at 680 mV vs. Ag/AgCl (Fig. 5B), close to that indicated before.

In this case, laccase molecules adsorbed through weak interactions should contain copper atoms with an electronic state much closer to that of the native molecule. It is worth noting that no reduction peaks were detected during the reverse potential scanning, because after its oxidation the enzyme is desorbed from the electrode surface.
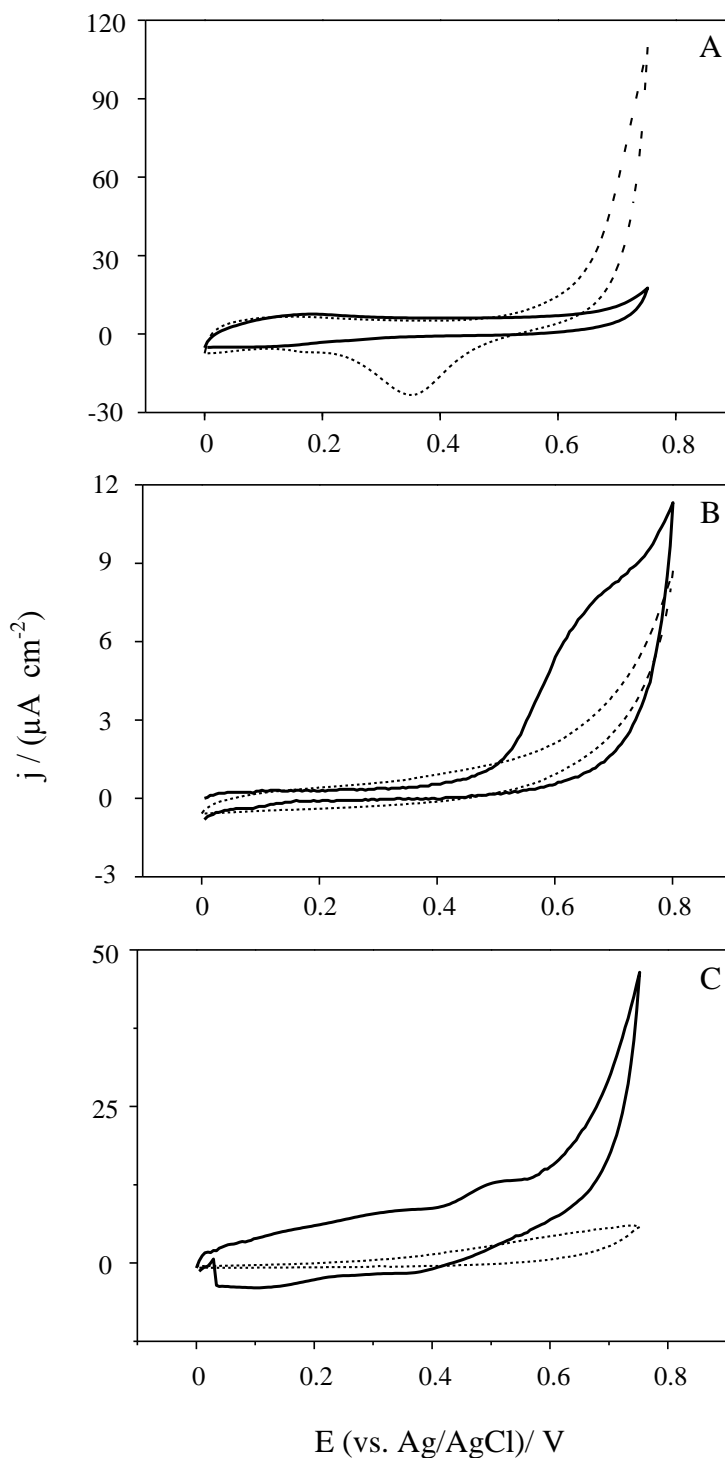
**Figure 5.** Cyclic voltammograms recorded in McIlvaine buffer (pH 6) of a laccase SML obtained on (A) Au, (B) HOPG, basal plane, and (C) SAM-Au. Dotted lines show the response of bare surfaces and solid lines correspond to the signal obtained for laccase SML. 0.050 V s$^{-1}$, in anaerobic atmosphere.

This event was also described for laccase multilayers physically adhered on HOPG [18]. By modifying the gold surface with an HDT-SAM (Fig. 5C), preventing the strong laccase-gold

interaction, the CV for the corresponding laccase SML again recovers the expected electrochemical response, and an anodic wave signal was detected at about 500 mV vs. Ag/AgCl. In this case a weak reduction wave is detected, which indicates the presence of the laccase bound to the thiol (Fig. 5B-C).

## 4. CONCLUSIONS

The molecular arrangements of the laccase SML and its electrochemical and catalytic behavior on gold and carbon electrode surfaces are linked to the corresponding laccase-surface interactions, and not necessarily, as widely thought, with a specific orientation of the enzyme on such surfaces. Despite working in sub-monolayer conditions which require extremely low enzyme concentrations, it was able to detect catalytic and electrochemical activity on HOPG and SAM-Au electrodes. However, under any test conditions we could no detect a specific orientation related to the type of electrode used as shown by the AFM and STM studies here presented. Therefore, a preferential orientation of the T1 or T2 (T2/T3 cluster) centers of the enzyme facing respectively the carbon or gold electrode surfaces is unlikely to be related with different enzymatic behavior. Even considering that the T1 center of the laccase must keep a determined distance from the electrode surfaces to allow fast electron transfer, our results for a laccase SML directly adhered on gold are evidence that the strong laccase-gold interactions are responsible for impairing the normal IET process in the enzyme. Consequently the laccase SML cannot perform its DET with the electrode, its catalytic effect being negligible, as we shown. In contrast, the weak interaction with HOPG and HDT-Au not only leads to a different arrangement of the laccase molecules but presumably permits a protein conformation compatible with a suitable IET process, conserving both catalytic activity and electrochemical response. These findings contribute to the knowledge of redox reactions carried out by laccase and therefore facilitate its applications in fields such as the development of biosensors and bio-fuel cells.

## References

1. A.L. Ghindilis, P. Atanassov and E. Wilkins, *Electroanalysis,* 9 (1997) 661.
2. J.R. Hernández Fernaud, A. Marina, K. González, J. Vázquez and M.A. Falcón, *Appl. Microbiol. Biotechnol.,* 70 (2006) 212.
3. D. Ivnitski and P. Atanassov, *Electroanalysis*, 19 (2007) 2307.
4. M. Klis, E. Maicka, A. Michota, J. Bukowskaa, S. Sek, J. Rogalski and R. Bilewicz, *Electrochim. Acta*, 52 (2007) 5591.
5. M.R. Duff and C.V. Kumar, *Langmuir*, 25 (2009) 12635.

6.  J.B. Lee, D.-J. Kim, J.-W Choi and K.-K. Koo, *Colloid Surf. B Biointerfaces*, 41 (2005) 163.

7.  S. Shleev, A. Christenson, V. Serezhenkov, D. Burbaev, A. Yaropolov, L. Gorton and T. Ruzgas, *Biochem. J.*, 385 (2005) 745.

8.  S. Shleev, A. Jarosz-Wilkolazka, A. Khalunina, O. Morozova, A. Yaropolov, T. Ruzgas and L. Gorton, *Bioelectrochemistry,* 67 (2005) 115.

9.  P. Ramírez, N. Mano, R. Andreu, T. Ruzgas, A. Heller, L. Gorton and S. Shleev, *Biochim. Biophys. Acta*, 1777 (2008) 1364.

10. L. dos Santos, V. Climent, C.F. Blanford and F.A. Armstrong, *Phys. Chem. Chem. Phys.*, 12 (2010) 13962.

11. E.I. Solomon, U.M. Sundaram and T.E. Machonkin, *Chem. Rev.*, 96 (1996) 2563.

12. L. Rulisek, E.I. Solomon and U.A Ryde, *Inorg. Chem.*, 44 (2005) 5612.

13. A. Christenson, S. Shleev, N. Mano, A. Heller and L. Gorton, *Biochim. Biophys. Acta*, 1757 (2006) 1634.

14. T. Sakurai, L. Zhan, T. Fujita, K. Kataoka, A. Shimizu, T. Samejima and S. Yamaguchi, *Biosci. Biotechnol. Biochem.*, 67 (2003) 1157.

15. S.K. Lee, S.D. George, W.E. Antholine, B. Hedman, K.O. Hodgson and E.I. Solomon, *J. Am. Chem. Soc.*, 124 (2002) 6180.

16. J. Yoon, B.D. Liboiron, R. Sarangi, K.O Hodgson, B. Hedman and E.I. Solomon, *Proc. Natl. Acad. Sci. U.S.A.*, 104 (2007) 13609.

17. F. Xu, W. Shin, S.H. Brown, J.A. Wahleithner, U.M. Sundaram and E.I. Solomon, *Biochim. Biophys. Acta*, 1292 (1996) 303.

18. K. González Arzola, Y. Gimeno, M.C. Arévalo, M.A Falcón and A. Hernández Creus, *Bioelectrochemistry*, 79 (2010) 17.

19. V. Regalado, A. Rodríguez, F. Perestelo, A. Carnicero, G. De la Fuente, M.A. Falcón, *Appl. Environ. Microbiol.*, 63 (1997) 3716.

20. K. González Arzola, O. Polvillo, M.E. Arias, F. Perestelo, A. Carnicero, F.J. González-Vila and M.A. Falcón, *Appl. Microbiol. Biotechnol.,* 73 (2006) 141.

21. U.K. Laemmli, *Nature*, 227 (1970) 680.

22. M.M. Bradford, *Anal. Biochem.*, 72 (1976) 248.

23. I. Horcas, R. Fernandez, J.M. Gomez-Rodriguez, J. Colchero, J. Gomez-Herrero and A.M. Baro, R*ev. Sci. Instrum.*, 78 (2007) 013705-1.

24. K.L. Shuttleworth, L. Posti and J.-M. Bollag, *Can. J. Microbiol.*, 32 (1986) 867.

25. V.A. Bogdanovskaya, M.R. Tarasevich, L.N. Kuznetsova, M.F. Reznik and E.V. Kasatkin, *Biosens. Bioelectron.,* 17 (2002) 945.

26. J.E.T. Andersen, M.H. Jensen, Per Moller and J. Ulstrup, *Electrochim. Acta*, 41 (1996) 2005.

27. H. Komori, K. Miyazaki and Y. Higuchi, *FEBS Lett.*, 583 (2009) 1189.

28. I. Matera, A. Gullotto, S. Tilli, M. Ferraroni, A. Scozzafava and F. Briganti, *Inorganica Chim. Acta*, 361 (2008) 4129.

29. M. Ferraroni, N.M. Myasoedova, V. Schmatchenko, A.A. Leontievsky, L.A. Golovleva, A. Scozzafava and F. Briganti, *BMC Struct. Biol.*, 7 (2007) 60.

30. M. Antorini, I. Herpoël-Gimbert, T. Choinowski, J.-C Sigoillot, M. Asther, K. Winterhalter and K. Piontek, *Biochim. Biophys. Acta*, 1594 (2002) 109.

31. T. Bertrand, C. Jolivalt, P. Briozzo, E. Caminade, N. Joly, C. Madzak and C. Mougin, *Biochemistry*, 41 (2002) 7325.

32. K. Piontek, M. Antorini and T. Choinowski, *J. Biol. Chem.*, 277 (2002) 37663.

33. V. Ducros, A.M. Brzozowski, K.S. Wilson, P. Østergaard, P. Schneider, A. Svendson and G.J. Davies, *Acta Cryst.*, D57 (2001) 333.

34. S. Shleev, Y. Wang, M. Gorbacheva, A. Christenson, D. Haltrich, R. Ludwig, T. Ruzgas and L. Gorton, *Electroanalysis*, 20 (2008) 963.

35. M. Pita, S. Shleev, T. Ruzgas, V.M. Fernández, A.I. Yaropolov and L. Gorton, *Electrochem. Commun.*, 8 (2006) 747.
36. C.F. Blanford, C.E. Foster, R.S. Heath and F.A. Armstrong, *Faraday Discuss.*, 140 (2009) 319.
37. H. Qiu, C. Xu, X. Huang, Y. Ding, Y. Qu and P. Gao, *J. Phys. Chem. C*, *113* (2009) 2521.
38. M. Aufray, A.A. Roche, *Appl. Surf. Sci.*, 254 (2008) 1936.
39. L. Venkataraman, J.E. Klare, I.W. Tam, C. Nuckolls, M.S. Hybertsen and M.L. Steigerwald, *Nano Lett.*, 6 (2006) 458.
40. A. Kumar, S. Mandal, P.R. Selvakannan, R. Pasricha, A.B. Mandale and M. Sastry, *Langmuir,* 19 (2003) 6277.
41. S. Bentadjine, R. Petiaud, A.A. Roche and V. Massardier, *Polymer*, 42 (2001) 6271.
42. D.V. Leff, L. Brandt and J.R. Heath, *Langmuir*, 12 (1996) 4723.
43. D. Ivnitski, K. Artyushkova and P. Atanassov, *Bioelectrochemistry*, 74 (2008) 101.
44. K. Haberska, C. Vaz-Domínguez, A.L. De Lacey, M. Dagys, C.T. Reimann and S. Shleev, *Bioelectrochemistry*, 76 (2009) 34.
45. S. Shleev and T. Ruzgas, *Angew. Chem.*, 120 (2008) 7380.
46. D.L. Johnson, J.L. Thompson, S.M. Brinkmann, K.A. Schuller and L.L. Martin, *Biochemistry*, 42*, (2003) 10229.
47. E.I. Solomon, R.K. Szilagyi, G.S. DeBeer and L. Basumallick, *Chem. Rev.*, 104 (2004) 419.
48. T.E. Machonkin and E.I. Solomon, J. *Am. Chem. Soc.*, 122 (2000) 12547.